

IMPROVEMENTS ON SEMI-CLASSICAL DISTORTED-WAVE MODEL

Sun Weili^{a),*}, Y. Watanabe^{a)}, R. Kuwata^{a)}, M. Kohno^{b)}, K. Ogata^{c)}, and M. Kawai^{c)}

^{a)}Dept. of Energy Conversion Engineering, Kyushu University, Kasuga 816, Fukuoka, Japan

^{b)}Physics Division, Kyushu Dental College, Kitakyushu 803, Japan

^{c)}Dept. of Physics, Kyushu University, Hakozaki, Fukuoka 812, Japan

* email: sun@ence.kyushu-u.ac.jp

Abstract A method of improving the Semi-Classical Distorted Wave (SCDW) model in terms of the Wigner transform of the one-body density matrix is presented. Finite size effect of atomic nuclei can be taken into account by using the single particle wave functions for harmonic oscillator or Wood-Saxon potential, instead of those based on the local Fermi-gas model which were incorporated into previous SCDW model. We carried out a preliminary SCDW calculation of 160 MeV (p,p'x) reaction on ⁹⁰Zr with the Wigner transform of harmonic oscillator wave functions. It is shown that the present calculation of angular distributions increase remarkably at backward angles than the previous ones and the agreement with the experimental data is improved.

1. Introduction

Dynamical nuclear processes, such as multistep direct (MSD) processes, become dominant in nuclear reactions at intermediate energies more than several tens of MeV. The semi-classical distorted wave (SCDW) model [1,2,3] had been proposed to describe the MSD processes and applied to analyze (p,p'x) reactions on medium-heavy nuclei for incident energies of 65 to 200 MeV. Previous calculations showed that this model succeeded in giving overall good agreement with the experimental angular distributions in the intermediate angular region, but failed to reproduce them at very forward and backward angles. Based on the consideration that the shape of MSD angular distributions is sensitive to the momentum distribution of target nucleons[4], it is supposed that the failure is due to the incorporation of a simple local Fermi-gas (LFG) model into SCDW model to describe the nuclear states, rather than the semi-classical approximations made in the SCDW model.

The LFG model can not properly take into account higher momentum components above the Fermi momentum. In ref. [5], it was indicated that the 1-step cross section drops steeply at the very forward and backward angles if no higher momentum component of nucleons is considered. This situation is similar to the above-mentioned SCDW results. To take into account the higher momentum components, one needs to use more realistic single-particle wave functions, such as that of the shell-

model potential. The Wigner transform of one body density matrix [6] is a proper tool of taking account of such single wave functions, while the characteristic features of the SCDW model keep unchanged, *i.e.*, a closed formed expression in coordinate representation which allows an intuitive interpretation of the MSD reaction. In this present work, we have reformulated the SCDW model in terms of the Wigner transform on the basis of the discussions in ref. [4], and carried out a preliminary calculation of $^{90}\text{Zr}(p,p',x)$ angular distributions at 160 MeV by using the Wigner transform of harmonic oscillator wave functions.

2. Formulation and methods of calculation

2.1 Wigner Transforms

We start from the Wigner transform $f(\mathbf{k}, \mathbf{r})$ of one-body mixed density for a j-j coupling single particle model with the wave functions $\phi_{n\ell jm}(\mathbf{x}, \boldsymbol{\sigma})$:

$$f(\mathbf{k}, \mathbf{r}) = \sum_{n\ell j} f_{n\ell j}(\mathbf{k}, \mathbf{r}), \quad (1)$$

where \mathbf{k} denotes the momentum of nucleon, \mathbf{r} the radius, and the sum is over all single particle orbits of target nucleons. The partial Wigner transform is

$$f_{n\ell j}(\mathbf{k}, \mathbf{r}) = \sum_m \int d\boldsymbol{\sigma} \int_0^\infty ds \exp(-i\mathbf{k}\mathbf{s}) \sum \phi_{n\ell jm}(\mathbf{r} + \mathbf{s}/2, \boldsymbol{\sigma}) \phi_{n\ell jm}^*(\mathbf{r} - \mathbf{s}/2, \boldsymbol{\sigma}), \quad (2)$$

where

$$\phi_{n\ell jm}(\mathbf{x}, \boldsymbol{\sigma}) = x^\ell u_{n\ell j}(x) [Y_\ell(\hat{\mathbf{x}}), \Psi_{1/2}(\boldsymbol{\sigma})]_{jm}, \quad (3)$$

where $\boldsymbol{\sigma}$ represents the spin of nucleon and $\Psi_{1/2}(\boldsymbol{\sigma})$ the spin function. The radical part $u_{n\ell j}(x)$ is expanded in terms of Gaussian basis:

$$u_{n\ell j}(x) = \sum_{v=1}^N a_v^{(n\ell j)} \exp(-\kappa_v^2 x^2). \quad (4)$$

The expansion coefficients $a_v^{(n\ell j)}$ is obtained by solving the Schrödinger equation with a finite potential, such as a harmonic oscillator (h.o.) potential or a Woods-Saxon potential through a variation method.

Using the above definitions, the final expression of the partial Wigner transform for a filled j-subshell is given:

$$\begin{aligned} f_{n\ell j}(\mathbf{k}, \mathbf{r}) = & (-)^\ell (2j+1) \sum_{v,v'=1}^N a_v^{(n\ell j)} a_{v'}^{(n\ell j)*} \exp(-(\kappa_v^2 + \kappa_{v'}^2)r^2) \sum_{L=even}^\infty i^L P_L(\cos\vartheta) \\ & \times \sum_{\lambda_1=0}^\ell \binom{2\ell+1}{2\lambda_1}^{1/2} r^{\ell-\lambda_1} \sum_{\lambda_2=0}^\ell \binom{2\ell+1}{2\lambda_2}^{1/2} r^{\ell-\lambda_2} (\ell - \lambda_1)(\ell - \lambda_2) \end{aligned}$$

$$\begin{aligned}
& \times \sum_{M=even}^{\infty} (2M+1) \sum_{\lambda} (-)^{\lambda+\lambda_1} (\lambda 0 M 0 | L 0)^2 W(\ell - \lambda_1 \lambda_1 \ell - \lambda_2 \lambda_2; \ell \lambda) \\
& \times (\ell - \lambda_1 0 \ell - \lambda_2 0 | \lambda 0) (\lambda_1 0 \lambda_2 0 | \lambda 0) I(\ell, \lambda, L, M, \lambda_1, \lambda_2; \kappa_v, \kappa'_v, k, r), \quad (5)
\end{aligned}$$

where: $I(\ell, \lambda, L, M, \lambda_1, \lambda_2; \kappa_v, \kappa'_v, k, r)$

$$= \int_0^{\infty} s^2 ds [\exp(-(\kappa_v^2 + \kappa'_v{}^2) \frac{s^2}{4}) j_L(ks) (\frac{s}{2})^{\lambda_1+\lambda_2} i_M((\kappa_v^2 - \kappa'_v{}^2)rs)], \quad (6)$$

where $P_L(\cos \vartheta)$ is Legendre function, ϑ represents the angle between momentum \mathbf{k} and radius \mathbf{r} . $j_L(x)$ and $i_M(x)$ are spherical Bessel and modified spherical Bessel functions, respectively, $(\lambda_1 0 \lambda_2 0 | \lambda 0)$ is Clebsh-Gorden coefficient and W the Racah coefficient.

It should be noted that the above derivation of Wigner transform is general. The sum over orbits in eq. (1) includes two parts, the contributions of all proton orbits and that of all neutron orbits, respectively. In present work, however, the distinction between proton and neutron is not considered, because the Coulomb potential for proton is neglected. In this situation the contribution of proton orbits with the same quantum numbers $n \ell j m$ as neutrons orbits is equal to that of neutron orbits.

2.2 SCDW model with Wigner transform:

The SCDW model and its related formulae had been given in detail elsewhere [1-3]. The Wigner transform can be incorporated into the SCDW model through the kernel $K^{(c)}(\mathbf{r}, \mathbf{r}')$ (c denotes proton or neutron shell) as discussed in ref. [4]:

$$K^{(c)}(\mathbf{r}, \mathbf{r}') \approx \frac{1}{(2\pi)^6} \int d\mathbf{k} d\mathbf{k}' e^{i\mathbf{q}(\mathbf{r}-\mathbf{r}')} f^{(c)}(\mathbf{k}, \mathbf{R})(1 - f^{(c)}(\mathbf{k}', \mathbf{R})) \delta(\hbar^2 k'^2 / 2\mu - \hbar^2 k^2 / 2\mu - \omega), \quad (7)$$

$$f^{(c)}(\mathbf{k}, \mathbf{R}) = \frac{1}{2} \sum_{n \ell j}^{(c)} f_{n \ell j}(\mathbf{k}, \mathbf{R}), \quad (8)$$

where $\mathbf{R} = (\mathbf{r} + \mathbf{r}') / 2$. The factor $1/2$ in eq.(8) comes from the consideration of spin of nucleon. As a result, the expression of the local average scattering cross section contains only an additional factor $f^{(c)}(\mathbf{k}, \mathbf{R})(1 - f^{(c)}(\mathbf{k}', \mathbf{R}))$ which stands for the probability of the state with momentum \mathbf{k} being occupied and the one with \mathbf{k}' being unoccupied. The other quantities used in the final SCDW expressions keep same. Thus, the present SCDW model with the Wigner transform still gives a simple closed-form expression of cross sections as before.

3. Results and Discussions

As an example, we calculated the Wigner transform and momentum distribution at harmonic oscillator (h. o.) and Woods-Saxon potential for ^{90}Zr . The number of Gaussian basis was taken as 10 which was enough to ensure the stability of Wigner transform against an increase in the number of

basis. The Clebsh-Gorden and Racah coefficients were calculated by standard subroutines. The h. o. parameter is $\hbar\omega_0=10$ and the depth is -55 MeV. The Woods-Saxon potential is of global type [7].

The calculated Wigner transforms for both potentials are shown in the three-dimensional plot in Figs. 1 and 2. It is found that each Wigner transform varies smoothly with increasing radius r or momentum k when ϑ is fixed. Note that the present numerical results of Wigner transform for h. o. potential is identical to the analytical results given in ref. [8].

In Figs. 3 and 4, the momentum distributions $n(k) = 1/(2\pi)^3 \int d\mathbf{r} f(\mathbf{k}, \mathbf{r})$ for both potentials are compared with those given by the simple Fermi-gas (FG) model, the LFG model and the QMD calculations[5]. The momentum distributions for both potentials contain a higher momentum tail and converge at $k=0$. Thus, it was found that the finite size effect of a nucleus improves remarkably the momentum distribution given by the LFG model which is divergent at $k=0$ and has no higher momentum components above the Fermi momentum. It is interesting to note that, as can be seen in Fig.4, there appears a difference between the momentum distributions for the h.o. potential and the Woods-Saxon potential in the high momentum region above the Fermi momentum: the former drops steeply, but the latter includes a tail extended towards the higher momentum region.

In terms of the Wigner transform, the higher momentum component of target nucleons caused by the finite size effect can be incorporated into the SCDW model. A preliminary calculation of angular distributions of the 160MeV(p,p'x) reaction on ^{90}Zr was carried out using the Wigner transform of h. o. wave functions. The basic input physical quantities, such as the distorting potentials, the N-N scattering cross sections, were kept same as the previous calculations [2].

Figs. 5 and 6 show comparisons of the present results with the previous calculations made with the LFG model. The calculation with the LFG model is in overall agreement with the experimental data in the intermediate angular region from about 30 to 60 degree, but the 1-step cross sections are almost zero at very small angles and drops steeply at backward angles. It can be seen that the use of the h.o. single-particle wave functions leads to remarkable increase not only in the 1-step cross section but also in the 2- and 3-step cross section at backward angles. Although the sum underestimates the experimental data for the lower emission energy, the result is very promising. Thus, it can be concluded that the finite size effect is one of the reasons why the angular distributions underestimate the experimental data at backward angles. We expect that the above calculations will be improved further if the Woods-Saxon potential is used because the higher momentum tail is contained as shown in Fig.4.

4. Summary

We have presented a method of improving the SCDW model in terms of the Wigner transform of the one-body density matrix. The improved SCDW model was applied to the calculation for the 160 MeV (p,p'x) reaction on ^{90}Zr . The preliminary result was very promising and indicated that the finite size effect is important to improve the agreement with the experimental data at backward angles.

However, there still appears somewhat underestimation at backward angles. This would require us to consider either higher order contributions above 3-step process or higher momentum components of target nucleons. SCDW calculations using the Woods-Saxon potential are now in progress in order to investigate the latter effect before time-consuming calculations for higher order contributions above 3-step process are carried out. Also, we intend to investigate how the single-particle wave functions in the surface region of nucleus affect nucleon emission to very small angles in order to give a satisfactory explanation for the rapid fall-off of the 1-step cross section seen around zero degree.

Acknowledgment

This work is partly supported by Grand-in-Aid Scientific Research of the Ministry of Education, Science and Culture (No. 07640416).

References

- [1] Y.L.Luo and M.Kawai, Phys.Rev. C 43, 2367 (1991)
- [2] Y. Watanabe and M.K.Kawai, Nucl. Phys. A 560, 43(1993)
- [3] M.Kawai and H.A.Weidenmuller, Phys.Rev. C 45, 1856 (1992)
- [4] M.Kawai, Y.Watanabe,H.Shinohara, M.Higashi, and M.Kohno, *Proceedings of the Fifteenth International Workshop on Nuclear Theory*, Rila mountains, Sofia, Bulgaria, 10-16 June, 1996
- [5] S.Chiba, M.B.Chadwick. K. Niita, T.Maruyama and A. Iwamoto, Phys. Rev. C 53, 1824(1996)
- [6] See, for example, H.Feshbach, *Theoretical Nuclear Physics, Nuclear Reactions* (John Wiley and Sons, 1992)
- [7] A. Bohr and B.R.Mottelson, *Nuclear Structure*, Vol.1, (W.A. Benjamin, Inc. New York, 1969), p.238
- [8] J. Martorell and E.Moya De Guerra, Annual of Physics 158, 1 (1984)

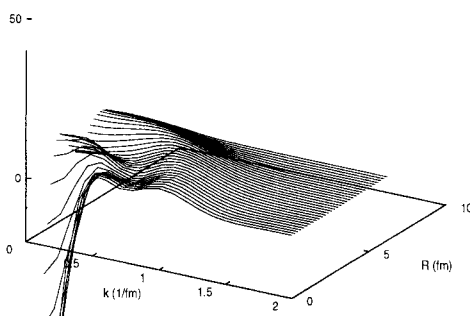


Fig.1 Wigner transform $f(k,r)$ at $\vartheta=0$
for Woods-Saxon potential

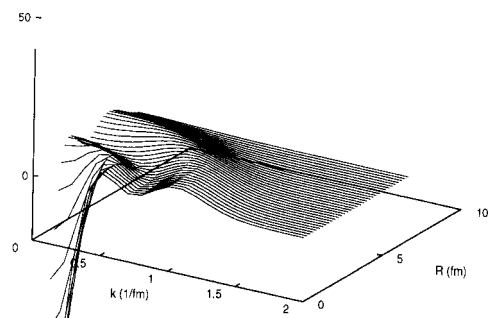


Fig.2 . Wigner transform $f(k,r)$ at $\vartheta=0$
for h. o. potential

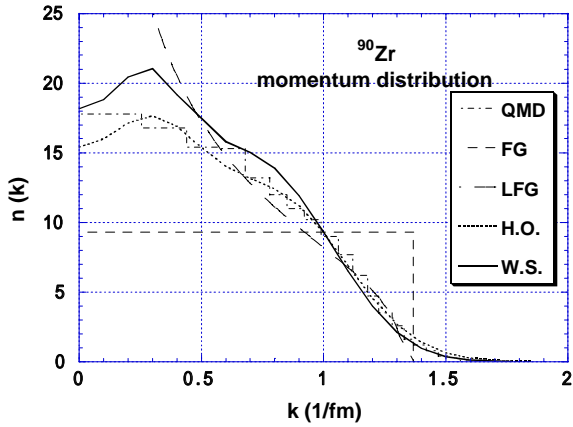


Fig.3 Momentum distribution for ^{90}Zr , (linear)

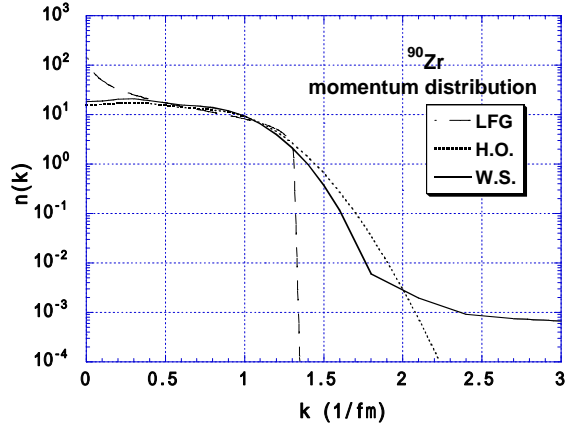


Fig.4 Momentum distribution for ^{90}Zr (logarithmic)

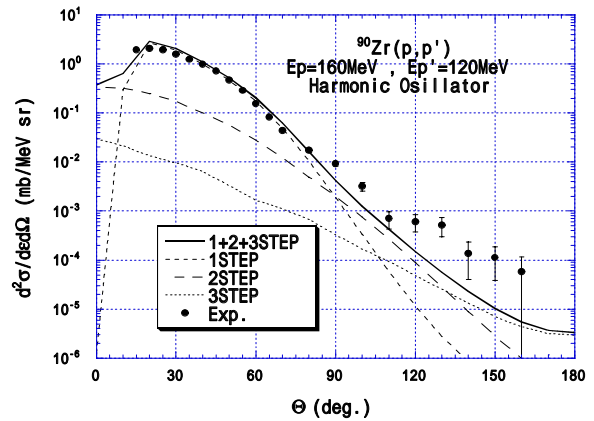
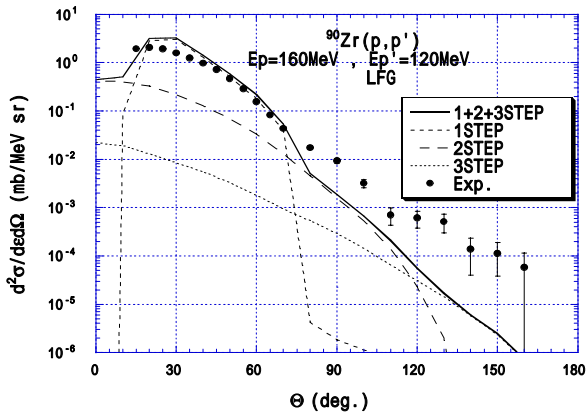


Fig.5 Comparison of calculated angular distributions with experimental data for $^{90}\text{Zr}(p,p')$ reaction at an incident energy of 160 MeV and an outgoing energy of 120 MeV. The left and right ones are calculated by SCDW model with LFG model and that with the Wigner transform for the harmonic oscillator potential, respectively.

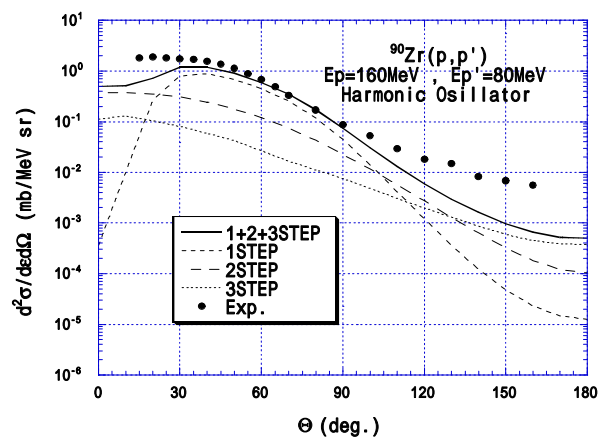
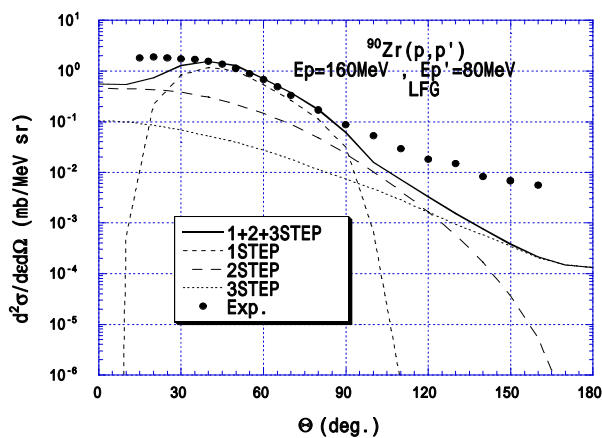


Fig.6 Same as in Fig.5, but for an outgoing energy of 80 MeV